

Prabhakar Palni, on behalf of the CDF Collaboration^a

^a*Department of Physics and Astronomy, University of New Mexico, MSC07 4220, 1919 Lomas Blvd. NE, Albuquerque, NM 87131-0001, USA*

Abstract

Using data from $p\bar{p}$ collisions at $\sqrt{s} = 1.96$ TeV recorded by the CDF II detector at the Fermilab Tevatron, we present three recent results on heavy flavor production: an observation of the excited resonance state Λ_b^{*0} in its fully reconstructed decay mode to $\Lambda_b^0\pi^+\pi^-$, a study of quark fragmentation using kaons produced in association with prompt D_s^\pm/D^\pm mesons, and the measurement of angular distributions of muons from $\Upsilon(1S, 2S, 3S)$ decays in both the Collins-Soper and the s -channel helicity frames.

1. Observation of the bottom baryon resonance Λ_b^{*0} (5920)

Baryons with a heavy quark Q as the nucleus and a light diquark q_1q_2 as the two orbiting electrons can be viewed as the helium atoms of QCD. The heavy quark in the baryon may be used as a probe of confinement which allows the study of non-perturbative QCD in a different regime from that of the light baryons.

The models that describe the heavy hadron's spectroscopy in the framework of Heavy Quark Effective Theories (HQET) [1] treat the heavy baryon as a system of a heavy quark Q considered as a static color source with mass $m_Q \gg \Lambda_{QCD}$ and a light diquark qq with a gluon field [2]. As the spin S_{qq} of the light diquark and the spin S_Q of the heavy quark are decoupled in HQET, heavy baryons can be described by the quantum numbers S_Q, m_Q, S_{qq} , and m_{qq} .

The total spins of the S -wave (no orbital excitations) baryon multiplets can be expressed as the sum $J = S_Q + S_{qq}$. Then the singlet Λ_b^0 baryon, with quark content $b[ud]$ according to HQET, has the spin of the heavy quark $S_b^P = \frac{1}{2}^+$ and isospin $I = 0$. Its flavor antisymmetric $[ud]$ diquark has the spin $S_{[ud]}^P = 0^+$ [3]. Under these conditions the b quark and the $[ud]$ diquark make the lowest-lying singlet ground state $J^P = \frac{1}{2}^+$. The partner of the Λ_b^0 baryon in the charm quark sector is the Λ_c^+ baryon.

Once the $[ud]$ diquark acquires an orbital excitation

with $L = 1$ relative to the heavy quark b , two excited states Λ_b^{*0} emerge with the same quark content as the singlet Λ_b^0 , with isospin $I = 0$ but with total spin $J^P = \frac{1}{2}^-$ or $J^P = \frac{3}{2}^-$. These isoscalar states are the lowest lying P -wave states that can decay to the singlet Λ_b^0 via strong processes involving emission of a pair of soft pions if parity P is conserved and provided sufficient phase space is available. Both Λ_b^{*0} particles are classified as bottom baryon resonant states.

LHCb has reported the first observation of two narrow structures at 5912 MeV/ c^2 and 5920 MeV/ c^2 [4] in the invariant mass spectrum of $\Lambda_b\pi^+\pi^-$. These structures are interpreted as the orbitally excited $\Lambda_b^{*0}(5912)$ and $\Lambda_b^{*0}(5920)$ bottom baryon resonances. Using a data sample of 9.6 fb $^{-1}$ collected with the CDF II detector [5], we undertake a search for the resonant states produced at the Tevatron and decaying in the same mode, $\Lambda_b\pi^+\pi^-$ [6].

This analysis is based on a CDF data set collected with the displaced two-track trigger [7] between March 2002 and December 2011. We search for Λ_b^{*0} states in the exclusive strong decay mode $\Lambda_b^{*0} \rightarrow \Lambda_b\pi^+\pi^-$, where the pair of low momentum pions $\pi^+\pi^-$ is produced near the kinematic threshold. The Λ_b^0 decays to $\Lambda_c^+\pi_b^-$, and this is followed by the weak decay $\Lambda_c^+ \rightarrow pK^-\pi^+$. To reconstruct the parent baryons, the tracks of charged particles are combined to form candidates. No particle identification is used in this analysis.

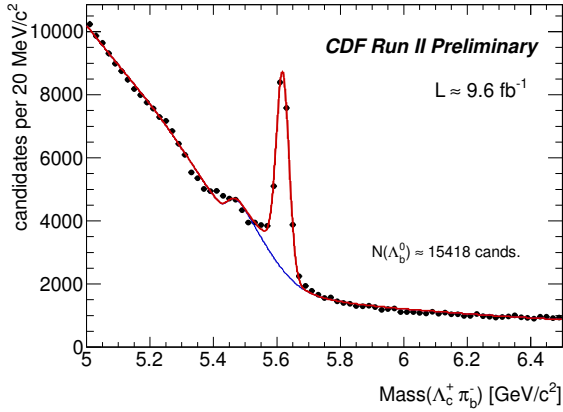


Figure 1: The invariant mass distribution of $\Lambda_b^{*0} \rightarrow \Lambda_b^0 \pi^+ \pi^-$ candidates with the projection of the mass fit overlaid.

The analysis begins with reconstruction of the $\Lambda_c^+ \rightarrow pK^- \pi^+$ decay by fitting three tracks to a common vertex. The invariant mass of the Λ_c^+ candidate is required to be within $\pm 18 \text{ MeV}/c^2$ of the world-average Λ_c^+ mass [8]. The momentum vector of the Λ_c^+ candidate is then extrapolated to intersect with a fourth track that is assumed to be the pion, to form the $\Lambda_b^0 \rightarrow \Lambda_c^+ \pi^-$ candidate. The Λ_b^0 vertex is subjected to a three-dimensional kinematic fit with the Λ_c^+ candidate mass constrained to its world average value.

To reduce combinatorial background and contributions from partially reconstructed decays, CDF requires the Λ_b^0 candidate's origin to be consistent with the primary vertex by requiring the impact parameter $d_0(\Lambda_b^0)$ not to exceed $80 \mu\text{m}$. The Λ_b^0 candidate must have transverse momentum $p_T(\Lambda_b^0)$ greater than $9.0 \text{ GeV}/c$ to ensure that the slow pions from the Λ_b^0 decay are within the kinematic acceptance of the track reconstruction. Figure 1 shows a prominent Λ_b^0 signal in the $\Lambda_c^+ \pi_b^-$ invariant mass distribution. A binned maximum-likelihood fit finds a signal of approximately 15,400 candidates at the expected Λ_b^0 mass, with a signal to background ratio of around 1.1. To reconstruct the $\Lambda_b^{*0} \rightarrow \Lambda_b^0 \pi^+ \pi^-$ candidates, each $\Lambda_c^+ \pi_b^-$ candidate with an invariant mass within the Λ_b^0 signal region, $5.561 - 5.677 \text{ GeV}/c^2$, is combined with a pair of oppositely charged tracks. The Λ_b^0 mass range covers ± 3 standard deviations as determined by a fit to the signal peak of Figure 1. The small bump below the Λ_b^0 signal corresponds to fully reconstructed B meson decays that pass the $\Lambda_b^0 \rightarrow \Lambda_c^+ \pi^-$ selection criteria.

To suppress systematic uncertainties, the analysis uses the mass difference Q , which is defined as

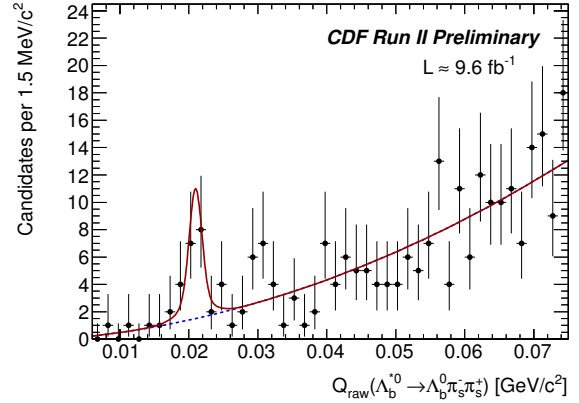


Figure 2: The projection of the unbinned fit for Q values of the Λ_b^{*0} candidates in the range $[0.006, 0.075] \text{ GeV}/c^2$.

$Q \equiv m(\Lambda_b^0 \pi^+ \pi^-) - m(\Lambda_b^0) - 2m(\pi^\pm)$. Figure 2 shows the result of a maximum likelihood fit to the unbinned Q -value distribution of Λ_b^{*0} overlaid with data. A narrow structure at $Q \sim 21 \text{ MeV}/c^2$ is clearly seen. The fit finds $17.3^{+5.3}_{-4.6}$ signal candidates at $Q = 20.68 \pm 0.35 \text{ MeV}/c^2$, where the resulting Q value is adjusted with the calibrated scale offset of $-0.28 \text{ MeV}/c^2$. From the measured Λ_b^{*0} Q value we extract the absolute masses using the known value of the π^\pm mass [8] and the CDF Λ_b^0 mass measurement, $m(\Lambda_b^0) = 5619.7 \pm 1.2 \text{ (stat)} \pm 1.2 \text{ (syst)} \text{ MeV}/c^2$, as obtained in an independent sample. The Λ_b^{*0} mass is found to be $m(\Lambda_b^{*0}) = 5919.5 \pm 0.35 \text{ (stat)} \pm 1.72 \text{ (syst)} \text{ MeV}/c^2$. The Λ_b^0 statistical and systematic uncertainties contribute to the systematic uncertainty on the Λ_b^{*0} absolute mass.

The local significance of the signal is 4.6σ . The significance of the signal for the search region of $6 - 50 \text{ MeV}/c^2$ is 3.5σ . The CDF result confirms the $\Lambda_b^{*0}(5920)$ state recently observed by the LHCb Collaboration. We do not observe the $\Lambda_b^{*0}(5912)$ resonance state observed by the LHCb Collaboration because of our low detector acceptance to slow pions. The result is consistent with theoretical predictions.

2. Quark fragmentation study using kaons produced in association with prompt D_s^\pm/D^\pm mesons

CDF probes the non-perturbative aspects of quark fragmentation by measuring the quark flavor fractions of charged particles produced in association with D_s^\pm and D^\pm mesons. Since QCD locally conserves quark flavor, this probes new details of the process by which quark anti-quark pairs are produced and subsequently

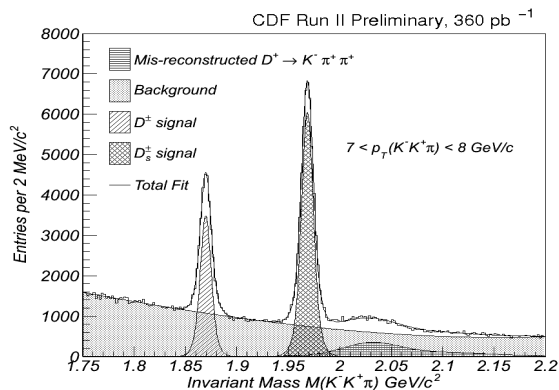


Figure 3: The invariant mass projections obtained from the likelihood fit performed in the lowest $p_T(KK\pi)$ bin.

form bound states in the fragmentation of a heavy quark jet. CDF has studied kaon production around charm mesons, namely D_s^\pm and D^\pm [9]. According to the naive fragmentation model, a kaon will be produced in the first fragmentation branch in association with a D_s^\pm , whereas creation of a D^\pm meson results in the production of a pion in the first fragmentation branch. Hence, more opposite-charge kaons are likely to be produced around D_s^\pm than D^\pm . In this study, we provide a comparison of the kinematical distributions of kaons produced around prompt D_s^\pm and prompt D^\pm that allows us to extract some information about the properties of the kaon that is most likely to be produced in the first fragmentation branch. We compare the results in data with predictions by the PYTHIA event generator [10] (which uses the string fragmentation model [11]) and with predictions by the HERWIG event generator [12] (which uses the cluster fragmentation model [13]).

Using a sample of events collected with a displaced two-track trigger [7], CDF reconstructs $D_s^\pm/D^\pm \rightarrow \phi\pi^\pm$, $\phi \rightarrow K^+K^-$ decays and analyzes events that have invariant mass in the range $1.75 < m(KK\pi) < 2.2$ GeV/c^2 . The particular trigger requires a pair of oppositely charged tracks with $p_T > 2.0$ GeV/c and impact parameter $d_0 > 120$ μm . The sum of their transverse momenta has to be greater than 5.5 GeV/c . This event sample, obtained from a data set of integrated luminosity 360 pb^{-1} , contains about $260,000$ D_s^\pm and $140,000$ D^\pm candidates with transverse momentum in the range $7 < p_T(KK\pi) < 30$ GeV/c .

To extract information pertaining to charm quark fragmentation, we concentrate on the prompt D_s^\pm/D^\pm component. We use the impact parameter distribution of the reconstructed $KK\pi$ candidates to statistically sep-

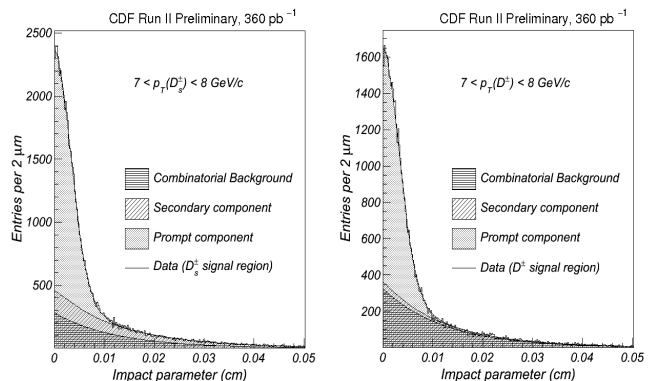


Figure 4: The impact parameter projections obtained from the likelihood fit performed in the lowest $p_T(KK\pi)$ bin.

arate the prompt and secondary D components in data. We use two particle identification techniques to measure the kaon, pion, and proton fractions around the various D components. These are the measurement of the specific ionization per unit track length (dE/dx) in the central tracking drift chamber and the time of flight of the particle measured in the Time-of-Flight (TOF) sub-detector. The silicon vertex trigger system has an excellent impact parameter resolution of 35 μm (50 μm when convoluted with a contribution from the beamspot).

A prompt D_s^\pm/D^\pm meson that is created during hadronization of the charm quark should ideally have zero impact parameter with respect to the primary vertex. However, due to the finite resolution of the detector, the impact parameter distribution of the prompt component will follow a Gaussian distribution with the width of the Gaussian being equal to the detector resolution. A secondary D_s^\pm/D^\pm meson that is produced in a B decay is boosted and can have nonzero impact parameter with respect to the primary vertex. This difference in the inherent shapes of the impact parameter distributions of the two components measured with respect to the primary vertex can be used to separate the prompt and secondary D_s^\pm/D^\pm components.

The invariant mass distribution is used to separate the D_s^\pm and D^\pm signal from the combinatorial background. The D_s^\pm and D^\pm signal peak is described using a double Gaussian function. The shape of the wide bump that occurs around 2.02 GeV/c^2 in the invariant mass distribution is obtained using Monte Carlo samples of mis-reconstructed $D^+ \rightarrow K^-\pi^+\pi^+$. A fourth order polynomial is used to describe the shape of the background component. The likelihood fit is performed in bins of transverse momentum of the $KK\pi$ candidate. The in-

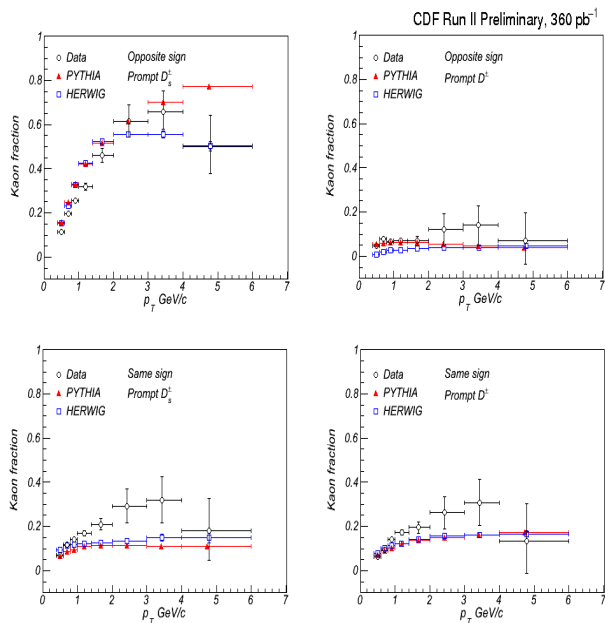


Figure 5: Distribution of kaon fractions measured around prompt D_s^\pm/D^\pm mesons in bins of transverse momentum p_T of the maximum- p_T track found in the cone. The data are compared to predictions by the PYTHIA and HERWIG generators for tracks of the same and opposite signs, for prompt D_s^\pm and D^\pm mesons.

variant mass projections obtained from the fit are shown in Fig. 3.

The shape of the prompt D component in the impact parameter distribution is described using a double Gaussian function. In order to describe the shape of the secondary component, we extract the impact parameter distribution of secondary D_s^\pm/D^\pm mesons using Monte Carlo samples of B decays. The template that describes the impact parameter distribution for secondary D_s^\pm/D^\pm is convoluted with the prompt resolution function. The shape of the background component in the impact parameter distribution is obtained empirically. The impact parameter of the background is assumed to be independent of mass, so we use the same function to describe the impact parameter of the background component in the sideband regions and under the D_s^\pm/D^\pm signal peaks, i.e., in the entire mass range $[1.75, 2.2]$ GeV/ c^2 . The impact parameter projections obtained from the likelihood fit to data within $\pm 3\sigma$ of the D_s^\pm/D^\pm signal peak are shown in Fig. 4.

We select the maximum- p_T track in a cone of radius $\Delta R = 0.7$ around the $(KK\pi)$ candidate, where $\Delta R = \sqrt{\Delta\eta^2 + \Delta\phi^2}$, η is pseudorapidity, and ϕ is azimuthal angle. This requirement is based on the hypoth-

esis that the maximum- p_T track is most likely to be correlated with the production of a heavy meson in the fragmentation process. Using the sample of maximum- p_T tracks, we measure the kaon fraction around the prompt D_s^\pm/D^\pm component by performing a multidimensional likelihood fit using four distributions: the invariant mass and impact parameter distributions of the $(KK\pi)$ candidates and the TOF and dE/dx distributions of the maximum- p_T track found in the cone around the reconstructed $(KK\pi)$ candidates.

We measure the kaon fraction around prompt D_s^\pm/D^\pm mesons for opposite-sign and same-sign charge combinations. In the opposite-sign combination, the track in the cone and the D candidate are oppositely charged. In this case, we expect the kaon production to be enhanced around prompt D_s^\pm compared to prompt D^\pm since formation of a prompt D_s^\pm meson requires conservation of strangeness in the first fragmentation branch. In the same-sign combination, the track in the cone and the D candidate have the same charge. In this combination, we expect the kaon production fraction to be similar around both the D_s^\pm and D^\pm mesons since same-sign kaons are likely to be produced in later branches of the fragmentation process. In addition to the two charge combinations, we measure the kaon fraction around prompt D_s^\pm/D^\pm mesons and compare the distribution in data with predictions by the PYTHIA and HERWIG Monte Carlo event generators. This comparison is shown in Fig. 5.

The data indicate that, in the opposite-sign charge combination, kaon production around prompt D_s^\pm is enhanced compared to production around prompt D^\pm . In the same-sign charge combination, kaon production around prompt D_s^\pm and prompt D^\pm is similar. The enhanced production of oppositely charged kaons around prompt D_s^\pm mesons is a feature of the phenomenological models used to describe the fragmentation process in Monte Carlo event generators. The results of the comparative study indicate that the p_T distributions for early fragmentation kaons produced around prompt D_s^\pm are in better qualitative agreement with predictions of fragmentation models compared to generic kaons that are produced in later fragmentation branches, for which the models underestimate the fraction of kaons.

3. Measurement of angular distributions of $\Upsilon(nS) \rightarrow \mu^+\mu^-$ decays

For more than a decade, the description of heavy quarkonium production at hadron colliders has proven to be challenging. Models that were constructed to accommodate the surprisingly large production cross sections of J/ψ and Υ mesons also make specific predic-

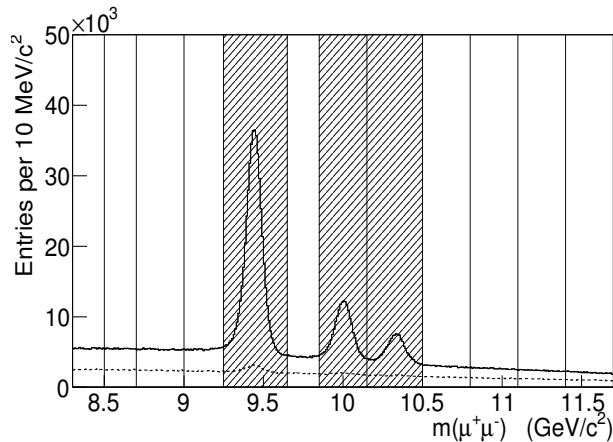


Figure 6: Mass distribution of $\mu^+\mu^-$ candidates in the prompt (solid line) and displaced (dashed line) samples, with the ranges of invariant mass used to select the signal and sideband events indicated. Hatched regions indicate the three mass ranges containing the $\Upsilon(nS)$ signals.

tions about their production polarization but are generally in poor agreement with experimental measurements [14, 15]. Discrepancies between results obtained by different experiments suggest that quarkonia might be strongly polarized when produced, but that different experimental acceptances limit formulation of a complete picture. The angular distribution of muons from $\Upsilon \rightarrow \mu^+\mu^-$ decays is described in the Υ rest frame by the distribution

$$\frac{d\Gamma}{d\Omega} \sim 1 + \lambda_\theta \cos^2 \theta + \lambda_\varphi \sin^2 \theta \cos 2\varphi + \lambda_{\theta\varphi} \sin 2\theta \cos \varphi, \quad (1)$$

where θ is the polar angle measured with respect to the quantization axis, and φ is the azimuthal angle measured with respect to the production plane containing the Υ and the beam axis. Previous experiments have only measured λ_θ as a function of the Υ transverse momentum in one reference frame, and significant polarization could be manifest by significantly nonzero values of λ_φ or $\lambda_{\theta\varphi}$ even when $\lambda_\theta \sim 0$ [16]. The CDF analysis employs a new technique with which to study the angular distribution of muons in Υ decay and is the first to provide information on all three coefficients, measured in multiple reference frames [17].

Using a sample of events collected with dimuon triggers, we reconstruct oppositely charged muons and analyze those events which have invariant mass in the range $8.3 < m(\mu^+\mu^-) < 11.7 \text{ GeV}/c^2$. This event sample, obtained from a data set of integrated luminosity 6.7 fb^{-1} , contains 550,000 $\Upsilon(1S)$, 150,000 $\Upsilon(2S)$, and 76,000

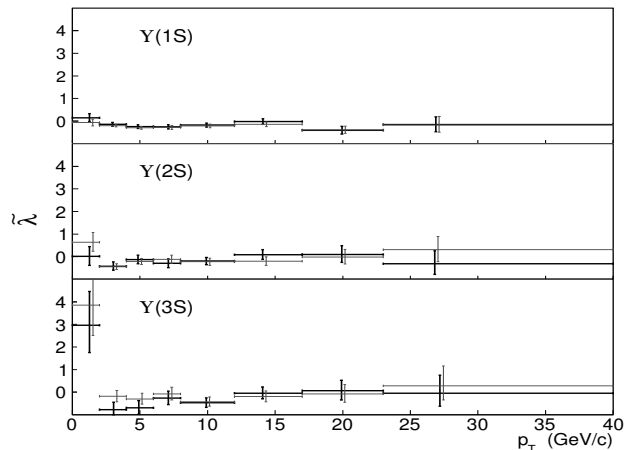


Figure 7: Rotational invariant $\tilde{\lambda}$ as a function of $p_T(\Upsilon)$ for the $\Upsilon(1S)$, $\Upsilon(2S)$, and $\Upsilon(3S)$ states.

$\Upsilon(3S)$ decays. The properties of dimuon candidates that have invariant mass near the $\Upsilon(nS)$ resonances are described using a two-component model for the $\Upsilon(nS)$ signal itself and the background. The angular distribution of the $\Upsilon(nS)$ component is extracted from the inclusive sample by means of constraints on the amount of background present in the sample and the angular distribution of the background component. We find that the background is dominated by muons from b -decays and can be suppressed by requiring that one muon is displaced, that is, has an impact parameter inconsistent with production at the primary vertex. We verify that this sample has the same angular distribution as the complementary prompt sample by comparing their angular distributions in mass regions that do not contain Υ decays.

The angular distribution analysis is performed separately in each of the 12 bins of dimuon mass shown in Fig. 6. The angular distributions of Υ decays are analyzed in eight bins of $p_T(\Upsilon)$ from 0 to 40 GeV/c and are restricted to rapidity $|\eta(\Upsilon)| < 0.6$. For a given range of transverse momenta, the sample of dimuon candidates is divided into two subsamples according to whether the trajectory of one of the muons misses the beam axis by a distance $|d_0| > 150 \mu\text{m}$. Events with at least one muon satisfying this requirement are referred to as the displaced sample since they are consistent with the presence of a long-lived parent particle, a characteristic feature of the dimuon background arising from semileptonic decays of heavy quarks. These criteria do not bias the angular distribution and, since the displaced sample contains almost no Υ signal, it provides a good descrip-

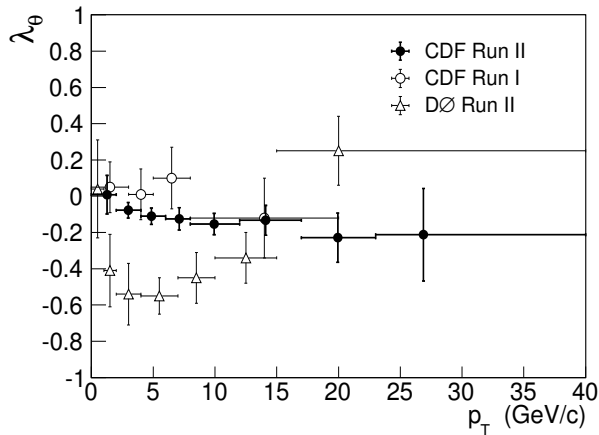


Figure 8: Comparison of the λ_θ parameter measured for $\Upsilon(1S)$ decays in the s -channel helicity frame with previous measurements from the CDF [14] and the D0 [15] experiments.

tion of the dimuon background that remains in the complementary prompt sample.

Figure 7 shows the rotational invariant $\tilde{\lambda}$, which is defined as $\tilde{\lambda} = \frac{\lambda_\theta + 3\lambda_\phi}{1 - \lambda_\phi}$. The rotational invariant is calculated from the measured values of λ_θ and λ_ϕ in each p_T range for both the Collins-Soper and s -channel helicity frames. Uncertainties in $\tilde{\lambda}$ measured in the two coordinate frames are highly correlated. Monte Carlo simulations are used to calculate the expected sizes of differences between the two values of $\tilde{\lambda}$ and in most cases, the observed deviations are found to be consistent with purely statistical fluctuations. The values of $\tilde{\lambda}$ suggest that the decays of all three $\Upsilon(nS)$ resonances are consistent with an unpolarized mixture of states.

Figure 8 shows a comparison of the λ_θ parameter, measured for the $\Upsilon(1S)$ state in the s -channel helicity frame, with previous measurements. The current result is found to be statistically consistent with the previous measurement from CDF [14], which was made for $|y| < 0.4$ at $\sqrt{s} = 1.8$ TeV. Restricting the current measurement to $|y| < 0.4$ does not change the results appreciably. The current $\Upsilon(1S)$ result is inconsistent with the previous measurement from the D0 experiment [15] at the level of 4.5σ .

4. Conclusions

CDF confirms the $\Lambda_b^{*0}(5920)$ state recently observed by the LHCb Collaboration. The local significance of the signal is 4.6σ , and the significance of the signal for the search region of $6 - 50$ MeV/ c^2 is 3.5σ . The result is consistent with theoretical predictions.

CDF compares the kinematic distribution of the measured kaon fraction around prompt D_s^\pm/D^\pm mesons with predictions from the string fragmentation model used in the PYTHIA event generator and the cluster fragmentation model used in the HERWIG event generator. The p_T distribution for early fragmentation kaons produced around prompt D_s^\pm is in good qualitative agreement with the predictions from the fragmentation models when compared to that of generic kaons that are produced in later fragmentation branches, for which the models underestimate the fraction of kaons.

We have measured the angular distributions of muons from $\Upsilon(1S)$, $\Upsilon(2S)$, and $\Upsilon(3S)$ decays with $|y| < 0.6$ and in several ranges of transverse momentum up to 40 GeV/ c . We find that the decay-angle distributions of all three $\Upsilon(nS)$ states are nearly isotropic, as was suggested by previous measurements [14] in the case of the $\Upsilon(1S)$. This is the first measurement to simultaneously determine the three parameters needed to fully quantify the angular distribution of $\Upsilon(nS) \rightarrow \mu^+\mu^-$ decays. This is also the first analysis to present information on the angular distribution of $\Upsilon(3S)$ mesons produced in high energy $p\bar{p}$ collisions. A recent CMS analysis employed the same technique and is in agreement with the CDF result [18].

References

- [1] M. Neubert, Phys. Rept. **245**, 259 (1994); A. V. Manohar and M. B. Wise, Camb. Monogr. Part. Phys. Nucl. Phys. Cosmol. **10**, 1 (2000).
- [2] N. Isgur and M. B. Wise, Phys. Lett. B **232**, 113 (1989); *Ibid.* **237**, 527 (1990).
- [3] J. G. Korner, M. Kramer, and D. Pirjol, Prog. Part. Nucl. Phys. **33**, 787 (1994).
- [4] R. Aaij *et al.* (LHCb Collaboration), arXiv:1205.3452 [hep-ex].
- [5] D. Acosta *et al.* (CDF Collaboration), Phys. Rev. D **71**, 032001 (2005).
- [6] CDF Collaboration, CDF public note 10900 (2012).
- [7] B. Ashmanskas *et al.* (CDF Collaboration), Nucl. Instrum. Meth. A **518**, 532-536 (2004).
- [8] J. Beringer *et al.*, Phys. Rev. D **86**, 010001 (2012).
- [9] CDF Collaboration, CDF public note 10704 (2012).
- [10] T. Sjostrand *et al.*, A Brief Introduction to PYTHIA 8.1, LU TP 07-28, October 2007.
- [11] B. Andersson *et al.*, Phys. Rev. Lett. **97**, 31 (1983).
- [12] G. Corcella *et al.*, HERWIG 6.5 Release Note, hep-ph/0210213.
- [13] D. Amati and G. Veneziano, Phys. Lett. B **83**, 87 (1979).
- [14] D. Acosta, *et al.* (CDF Collaboration), Phys. Rev. Lett. **88**, 161802 (2002).
- [15] V.M. Abazov, *et al.* (D0 Collaboration), Phys. Rev. Lett. **101**, 182004 (2008).
- [16] P. Faccioli *et al.*, Phys. Rev. D **81**, 111502(R) (2010).
- [17] T. Aaltonen *et al.* (CDF Collaboration), Phys. Rev. Lett. **108**, 151802 (2012).
- [18] S. Chatrchyan *et al.* (CMS Collaboration), arXiv:1209.2922 [hep-ex].